Metallurgical Engineering Department
Faculty of Petroleum and Mining Engineering

Design of High Entropy Superalloy FeNiCrAlCu with Stacking Fault Energy Modelling using Thermodynamic Calculation and Machine Learning

MG4090 – Final Project
Farrel Faiz Baskara – 12519056

Abstract – High entropy superalloys are promising class of material with unique properties, but their development and optimization remain ongoing. This study focuses on Fe-based high entropy superalloys and their stacking fault energy (SFE), a critical parameter influencing deformation mechanism and creep resistance. This development is economically cheaper since it's utilizing Fe element rather than Ni element which has been widely developed. Leveraging machine learning and computational thermodynamics, we propose a novel approach for predicting SFE using big data analysis. The simulation is carried out by determining the parameter used for thermodynamic calculation. These parameters are used to calculate SFE value by utilizing MATLAB software. The results of these calculation become the database for machine learning model. The model is built using TensorFlow especially using the Deep learning Neural Network (DNN) architecture. The model predicts the numerical values of SFE as well as their classes. Our research establishes an optimal design guide for achieving desired SFE values at 300 K: Ni (20-25 at%), Cr (15-36 at%), Al (5-20 at%), Cu (9-20 at%), and Fe (20-35 at%). Employing a deep learning neural network model, we achieve an impressive 0.008 Root Mean Squared Error in predicting SFE values and class. This work contributes to advancing high entropy superalloy design, providing valuable insights into their mechanical behavior, and enabling improved creep resistance for demanding applications.

Keywords: high entropy superalloy, stacking fault energy, machine learning

1 Introduction

Superalloys are nickel, iron-nickel and cobalt-based alloys that are often used as high-temperature material components, due to their excellent heat resistance properties [1]. Nickel-based superalloys are often relied upon in the energy, oil, gas and aviation sectors as key components of turbine engines [2], [3]. These superalloys rely on coherent dispersion of $Ni_3(Al,Ti)$-based $L1_2$ γ' precipitates in an fcc-γ matrix to produce high strength at high temperatures. In order to operate at higher temperatures, the addition of refractory elements such as Mo, W, Ta, Re, or Ru can form a superalloy capable of operating well above its melting temperature, as well as producing high creep resistance at high temperatures [4]. However, as refractory elements are expensive metals, their addition has the potential to limit the application range of such alloys.

In order to obtain better cost-performance alloys, high entropy alloys (HEA) allow the option of utilizing a wider compositional space [5]. High entropy alloys are a new class of materials with diverse multi-principal elements and interesting property-structure relationships [6]. HEA is defined to have at least 5 main elements ranging from 5 at% - 35 at%. High entropy is a term coined based on the idea that a single phase of a solid solution can be stabilized through a high entropy configuration or $|\Delta S_{mix}|$ value > 1.5 R [7], which is associated with random mixing of several elements with similar atomic fractions [8].

In its development, nickel-rich HEA became a breakthrough for the improvement of the thermal stability of the matrix γ and precipitated γ' phase microstructures that enabled the improvement of the alloy's strength at high temperatures. Nickel-rich HEAs with γ and γ' matrix microstructures resemble the microstructure of super alloys, so the material class is named High Entropy Superalloys (HESA) or high entropy super alloys [5]. HESA has the advantage of having low density and low manufacturing price compared to superalloys. In addition, HESA offers excellent high-temperature mechanical properties, such as high mechanical strength, corrosion resistance, oxidation resistance, and creep resistance [4]. The development of HESA involves superalloy elements such as Fe, Ni, Al, Ti, Cr, and Co, for example FeNiCoCrAl [9] and Fe45Ni25Cr-25Mo5-based alloys [10]. Given the relatively expensive elements Co and Mo, it is necessary to develop variations involving cheaper elements such as Cu. Cu has a relatively low price in alloy manufacturing [11], and the addition of Cu can also increase the toughness of the alloy [12]. FeNiCrAlCu is a new alloy development classified as iron-based HESA. This alloy has not yet been extensively analyzed for its properties and strength at elevated temperatures.

One of the key properties in materials that is very important to evaluate, especially in high temperature materials, is creep resistance [13]. Creep resistance refers to the ability of a material to withstand long-term loads or stresses at high temperatures [14]. Stacking Fault Energy (SFE) is one of the values that can describe the creep behavior of a material. SFE is defined as the energy required for the formation of a stacking fault per unit area in the atomic structure of the material. SFE can describe the deformation behavior of slip mode, twinning deformation, and martensitic transformation of a material [15]. A low SFE value means that the distance between two partial dislocations is wide, preventing complete dislocation so that cross slip is inhibited. Such events can restrain the creep rate.

The approach to measure the SFE value is usually done experimentally through the Transmission Electron Microscopy (TEM) method. The TEM method is theoretically a reliable method in SFE measurement, but there are several limitations such as measurements are difficult to perform and require a large amount of time and cost [16]. Computational methods have emerged as an alternative to approach the measurement of SFE values. Computational methods are methods used to design a metal alloy, by utilizing computer capabilities in simulating, calculating, and analyzing an alloy composition in order to achieve the desired microstructure and properties [17]. One example of a computational method is the first-principle density functional theory (DFT) method based on quantum mechanical theory. However, this method takes a relatively

long time to simulate and optimize. Therefore, machine learning methods are a new alternative to predict the SFE value of an alloy. Basically, the machine learning method requires large data in order to predict the SFE value, therefore the computational thermodynamics method is used to simulate the SFE value and the results become the database of the machine learning model.

In this study, the high entropy superalloy FeNiCrAlCu was simulated to obtain the SFE value. The simulation was carried out using computational methods based on thermodynamic calculations and machine learning. The results of the simulation were then analyzed to study the effect of the parameters used on the SFE value.

2 Simulation Procedure

A series of simulations were conducted to study the effect of composition and temperature variations on the Stacking Fault Energy (SFE) value of FeNiCrAlCu high entropy superalloy, using thermodynamic calculation and machine learning methods. Thermodynamic calculations using MATLAB software, and machine learning modeling simulations using Jupyter Notebook software with the help of TensorFlow. The results of the calculation of the SFE value from MATLAB are then used as a database to interpret the relationships and patterns that occur, and then become input for machine learning models that can learn patterns from the data, and predict value and class of the SFE. The simulation flowchart is briefly shown in Figure 1

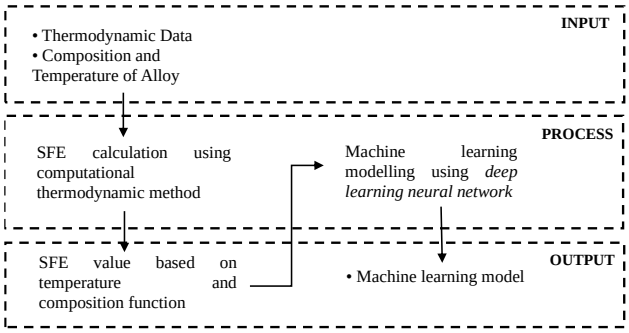

Figure 1 Flowchart of simulation in this study

2.1 Computational Thermodynamic Method

Stacking fault energy modelling considers the phenomenon of phase transformation change from γ-fcc to ε-hcp of the thin plate ($\Delta G^{\gamma\rightarrow\varepsilon}$) by involving the interface energy ($\sigma^{\gamma/\varepsilon}$), o that the intrinsic SFE value can be calculated:

$$\gamma_{sf} = 2\frac{4}{\sqrt{3}}\frac{1}{a^2 N}\Delta G^{\gamma\rightarrow\varepsilon} + 2\sigma^{\gamma/\varepsilon}$$

where γ_{sf} is the intrinsic SFE value (mJ/m^2), the initial equation $\frac{4}{\sqrt{3}}\frac{1}{a^2 N}$ is the value of atomic density (ρ), which is calculated with a as the lattice parameter and N is Avogadro's constant The value of the lattice parameter is a constant value of 3.58 Å assuming there is no dependence between the lattice parameter and composition and temperature. $\Delta G^{\gamma\rightarrow\varepsilon}$ is the difference in Gibbs free energy at the fcc to hcp phase transformation, $\sigma^{\gamma/\varepsilon}$ is the interface energy per unit area of the phase boundary. In a multi-component alloy, the equation is extended to include the change value of the Gibbs energy of each element i ($\Delta G_i^{\gamma\rightarrow\varepsilon}$), the excess bond energy between elements i and j ($\Delta\Omega_{ij}^{\gamma\rightarrow\varepsilon}$) as well as the magnetic contribution to the Gibbs free energy ($\Delta G_{mg}^{\gamma\rightarrow\varepsilon}$), which is then the Gibbs free energy equation is written as:

$$\Delta G^{\gamma\rightarrow\varepsilon} = \sum_i X_i \Delta G_i^{\gamma\rightarrow\varepsilon} + \sum_{ij} X_i X_j \Delta\Omega_{ij}^{\gamma\rightarrow\varepsilon} + \Delta G_{mg}^{\gamma\rightarrow\varepsilon}$$

with X_i being the mole fraction of the corresponding element of each alloy.

2.2 Machine Learning Method

The results of all thermodynamic calculations become the database of machine learning modeling. The database has a total of 2340 data with the feature or input is the atomic percent of each alloy composition and temperature, while the target or output is the SFE value. This modeling uses jupyter notebook software with the help TensorFlow, an end-to-end open-source platform for machine learning.

The modeling process begins by entering the results of thermodynamic calculations as input, then data preparation is carried out to retrieve the required features and targets. The data is then divided into training data and validation data with a ratio of 80:20. Training data is data that is used to train a model in order to understand the patterns and correlations between features and targets in the database. Meanwhile, validation data is data that has never been seen by machine learning models before, and is used to assess how accurate the predictions are. After that, the model is evaluated by comparing the prediction results by machine learning with the actual results, so that the model that has the best performance can be chosen. The flowchart of the modeling process is presented in Figure 2

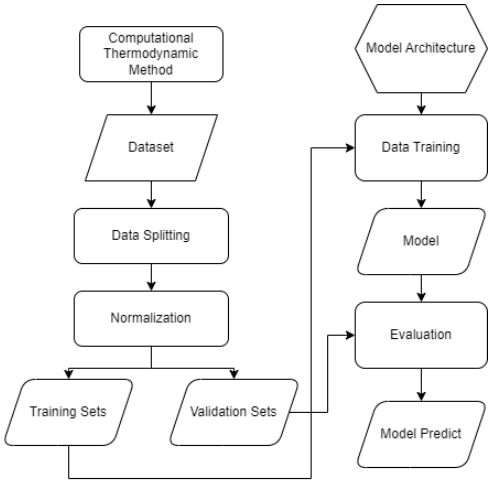

Figure 2 Flowchart of machine learning processes

The model is built using deep neural network architecture, trained in 10 epchs using adam optimizer and mean squared error loss function. After training, the model is evaluated using Root Mean Squared Error (RMSE) metrics. If the RMSE is good, then the model can be used for prediction.

3 Results and Discussion

3.1 Effects of Temperature on SFE

The results of temperature and SFE values are presented in Figure 3 to see the effect of increasing temperature on SFE. Based on the calculation, the SFE value increases with increasing temperature. This is due to the value of $\Delta G^{\gamma\rightarrow\varepsilon}$

which is a function of temperature, which means that the increase or decrease of the value depends on the temperature value.

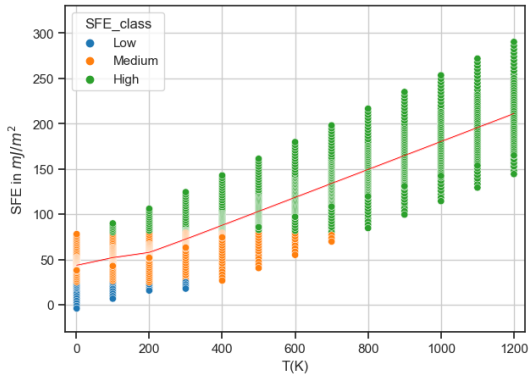

Figure 3 The effect of increasing temperature on SFE

Based on Gibbs energy equation which is $\Delta G = \Delta H - T\Delta S$, if the Gibbs energy function has a positive entropy value, then increasing the temperature will increase the $\Delta G_{chemical}$ value and therefore increase the SFE value. Conversely, if the entropy value is negative, an increase in temperature will decrease the SFE value. Similar results were also found in the study of iron-based alloys Fe-Cr-Ni system, conducted by Hojjat Gholizadeh[18] with the results showing an increase in SFE with increasing temperature. It was found that the effect of temperature on SFE is mainly influenced by lattice expansion and the driving force for hcp to fcc phase transformation. In addition, research conducted by Zhang et al [19], [20] through experiments using XRD, showed that the decrease in the SFE value of HEA CrCoFeMnNi alloy is due to the stabilization of the hcp phase at low temperatures, or in other words, the fcc phase is more stable with increasing temperature so that the SFE value increases.

3.2 Effects of Ni atom addition on SFE

The results of the thermodynamic calculations on the addition of Ni atoms to the SFE value are presented in Figure 4 Based on this figure, the increase in SFE occurs along with the increase in at%-Ni. For example, at a temperature of 300 K, the SFE increases from 56.35 mJ/m2 to 100.52 mJ/m2.

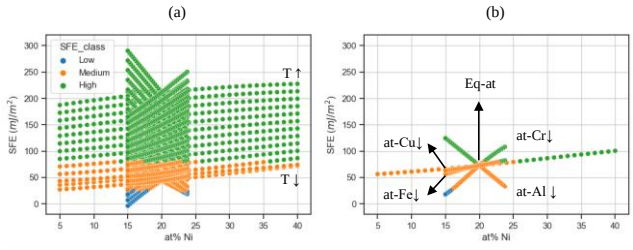

Figure 4 The effect of Ni atom addition on SFE

The tendency to increase the SFE value remains consistent as the temperature increases, on the graph, namely the distribution vertically upwards at one composition point. It is also shown that there is a branching that occurs according to the information in Figure 4 (b), namely as the Ni element increases, the other elements will decrease evenly. The decrease in each element has a different impact on the SFE value, such as a decrease in Fe, Cu, Cr increases SFE while a decrease in Al can reduce SFE.

The relationship between SFE and Ni in this study is similar to the research conducted by Wang et al [21]. In that study, it was proven through tensile testing of Cu-Ni alloys, with a range of Ni from 5-20% which showed that with an increase in Ni content, the SFE simultaneously. In addition, the same is also shown in the research conducted by Zhao et al [22], regarding the phase transformation in CoCrNix medium entropy alloy. The study analyzed that as the Ni content increases, the intensity of the hcp phase decreases, which according to thermodynamic calculations by Olson and Cohen, the SFE value will increase.

3.3 Effects of Cr atom addition on SFE

The results of thermodynamic calculations on the addition of Cr atoms to the SFE value are presented in Figure 5. Based on this figure, the decrease in SFE occurs along with the increase in at%-Cr, for example at a temperature of 300 K, the resulting decrease in SFE from 107.89 mJ/m2 to 17.97 mJ/m2.

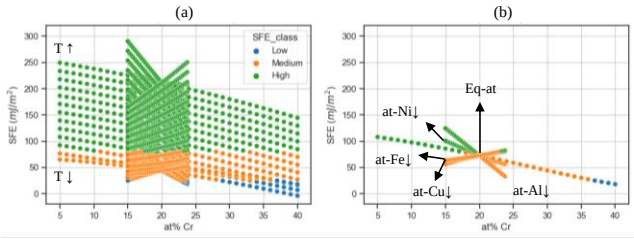

Figure 5 The effect of Cr atom addition on SFE

The tendency to decrease the SFE value remains consistent as the temperature increases, on the graph is a vertical distribution at one composition point, while the branching that occurs is the effect of other composition variations as in the description.

Similar results were also obtained in the article on the effect of element addition on stacking fault energy in Fe-Mn-C austenitic steel, by A. Dumay, et al [23]. In Fe¬22Mn0.6C steel alloy, it can be seen that the addition of Cr element decreases the SFE value. The tendency of Cr to reduce the SFE is also shown in the simulation conducted by Yan et al [24], with the Density Functional Theory (DFT) method on CoCrxNi and a decrease in the intensity of the hcp phase along with an increase in Cr atoms. In this study, the increase in Cr content is related to the deformation of thin twinning, and the first principle DFT calculation indicates a decrease in SFE which may contribute to the appearance of nano-twins. In summary, the role of Cr in plastic deformation is to increase nano-twins and slip bands that occur during tensile processing. The influence of TWIP is the reason for the good ductility of the alloy.

3.4 Effects of Al atom addition on SFE

The results of thermodynamic calculations on the addition of Al atoms to the SFE value are presented in Figure 6. Based on this figure, the increase in SFE occurs along with

the increase in at%-Al, for example at a temperature of 300 K, the resulting increase in SFE from 33.10 mJ/m2 to 124.42 mJ/m2.

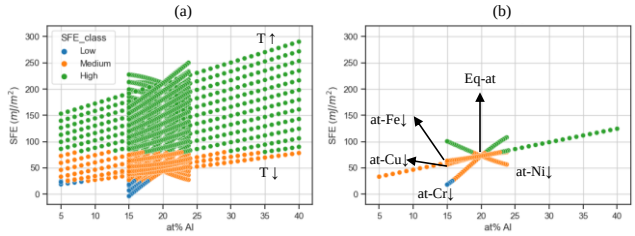

Figure 6 The effect of Al atom addition on SFE

The tendency to increase the SFE value remains consistent as the temperature increases, on the graph, the distribution is vertical at one point of the composition, while the branching that occurs is the effect of other composition variations as in the description.

Similar results were found in research conducted by Kyung-Tae Park et al [25] which showed the addition of Al to Fe-22Mn-xAl-0.6C austenitic steel can increase the SFE value. In the study, it is said that the increase in SFE due to the addition of Al can resist or delay the occurrence of mechanical twinning. In addition, research conducted by Sun et al [26] on HEA $Al_y(CrMnFeCoNi)_{1-y}$ alloy showed that the twinning ability of the alloy will decrease due to the addition of Al atoms and SFE will increase along with the addition of Al atoms. This reinforces previous research that with the addition of Al atoms, SFE will increase and twinning will be more difficult.

3.4 Effects of Cu atom addition on SFE

The results of thermodynamic calculations on the addition of Cu atoms to the SFE value are presented in Figure 7. Based on this figure, the decrease in SFE occurs along with the increase in at%-Cu, for example at a temperature of 300 K, the resulting decrease in SFE from 82.26 mJ/m2 to 63.18 mJ/m2.

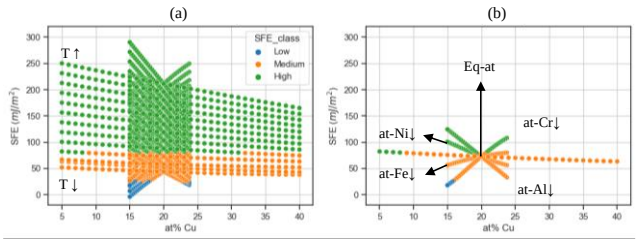

Figure 7 The effect of Cu atom addition on SFE

This tendency to decrease the SFE value also remains consistent as the temperature increases, on the graph i.e., the distribution is vertical at one composition point. At higher temperatures, the effect of Cu is also more significant than at lower temperatures, as indicated by the increasing slope. The bifurcation that occurs is the effect of other composition variations as in the description.

The decrease in SFE that occurs due to an increase in Cu atoms occurs insignificantly when compared to changes in other elements. According to research conducted by Lei Huang [27], the addition of Cu atoms as much as 0; 0.5; 1.0; 1.5; and 2.0 at% in AlCrFeNiTiCux alloy can increase the intensity of fcc. This means that as the Cu content in the alloy increases, the fcc stability will increase, and therefore the SFE increases. This can happen because in the simulation, there is an influence from other elements that is more dominant. Given the insignificant effect of Cu addition, the influence of other elements can be dominant in the overall SFE calculation.

3.5 Effects of Fe atom addition on SFE

The results of thermodynamic calculations on the addition of Fe atoms to the SFE value are presented in Figure 8. Based on this figure, the decrease and increase in SFE occurs along with the increase in at%-Fe. Increasing the percent of Fe atoms from 5 to 40 percent shows a decrease in SFE at temperatures of 1 K to 900 K, after which an increase in at%-Fe increases the SFE value. For example, at 300 K, the SFE decreases from 79.93 mJ/m2 to 56.14 mJ/m2, while at 1100 K, the SFE increases from 192.96 mJ/m2 to 195.19 mJ/m2.

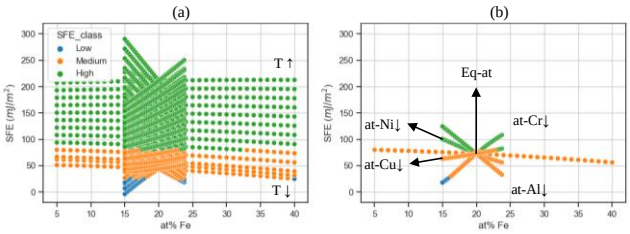

Figure 8 The effect of Fe atom addition on SFE

This can be explained according to thermodynamic calculations, where the value of $\Delta G_{Fe}^{\gamma \rightarrow \varepsilon}$ is a function of positive entropy, so as the temperature increases, the value will become positive at a certain point, and change its contribution to the SFE to be positive. This shows that the effect of SFE can vary depending on the temperature and composition of Fe.

However, in general, the addition of Fe tends to decrease the SFE, because Fe has a relatively low SFE value compared to other elements, and its presence in the crystal lattice can cause a reduction in the overall SFE. Research by Wang et al [28] gave similar results, with Fe-Cr alloys showing that the addition of Fe atoms can reduce the SFE value, and the greater the composition of Fe atoms in the alloy, the possibility of the alloy to undergo twinning deformation will increase as well.

3.7 Machine Learning Model Evaluation

In this section, we will discuss the performance of the machine learning model and compare the model prediction results with the thermodynamic calculation data and the calculation results with the first principle method by Ammar Zamani (2021) [29]. The evaluation carried out uses root mean squared error (RMSE).

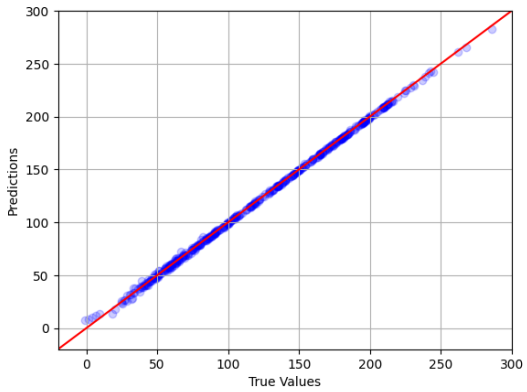

Figure 9 True values vs prediction values in linear graph

From figure 9 it can been seen that True values is aligning with the predictions value, means the model predict the value accurately, the R2 score for this model is 0.98. Other than that, the RMSE of this model are 0.005 for the training and 0.008 for the validation. This means the model is not overfitting since the validation is not below the training RMSE and not underfit since the training RMSE is already reaching small error.

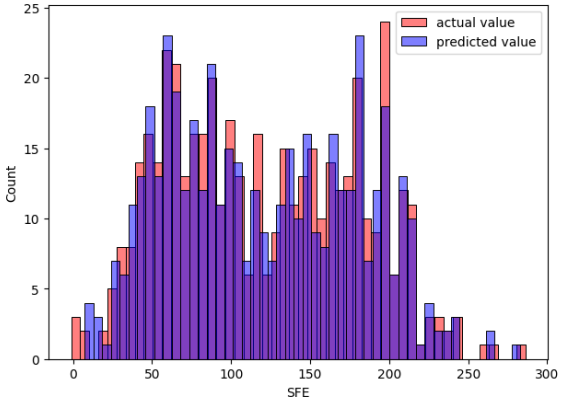

Figure 10 Actual and predicted value on models' evaluation

Figure 10 shows a visualization of how many the predicted value in each SFE values accurately predicted. The red bar indicates the actual value from the SFE calculated using computational thermodynamic method, and the blue bar indicates the predicted values. It's shown that the blue bar is covering up the red ones, means it's accurately predicted. Nevertheless, there is uncovered red bar which shows the error which model's yield.

The model then used to predict the SFE with new composition, and then compared with the thermodynamic and first-princilple method. Based on the data by Ammar Zamani [29], the value of FeNiCrAl alloy was calculated based on thermodynamic and first-principle methods and then compared with the prediction results of the machine learning model in this study. The comparison of the SFE values is shown in table 1.

Table 1 Comparison of Thermodynamical, First Principle, and Deeplearning Neural Network Results

T(K)	Paduan	SFE (mJ/m^2)		
		Termo	First Principle	DNN
0	$Fe_{25}Ni_{25}Cr_{25}Al_{25}$	55.22	52.22	52.89
0	$Fe_{25}Ni_{25}Cr_{30}Al_{20}$	40.86	24.51	39.16
0	$Fe_{25}Ni_{30}Cr_{25}Al_{20}$	56.82	72.2	55.48
T(K)	Paduan	SFE		
		Termo	First Principle	DNN
0	$Fe_{25}Ni_{25}Cr_{25}Al_{25}$	*Medium*	*Medium*	*Medium*
0	$Fe_{25}Ni_{25}Cr_{30}Al_{20}$	*Medium*	*Low*	*Medium*
0	$Fe_{25}Ni_{30}Cr_{25}Al_{20}$	*Medium*	*Medium*	*Medium*

Table 1 shows that the value of SFE produced by the machine learning neural network model can predict the value of SFE with results that are close to the value of thermodynamic calculations, but do not really represent the results in the first-principle calculation. This happens because the training data used to train the model is the result of thermodynamic calculations, so the model is not trained with the results of the first-principle method. However, in $Fe_{25}Ni_{25}Cr_{25}Al_{25}$ alloy the model is able to predict close to the first-principle value, of course this can happen because the value of thermodynamics is initially close to the value of the first-principle.

Therefore, the main difference that occurs here is the difference between the results of the thermodynamic calculation method and the first-principle method, which can occur for several reasons, including 1) Different method approaches, in the first-principle, SFE is measured with a quantum mechanical theory approach such as its atomic structure. While in thermodynamic calculations, the approach is done through Gibbs energy by Olson [37] and Cohen which is very dependent on temperature and alloy composition, and 2) Calculations at temperatures that are not exactly the same, because thermodynamic calculations cannot calculate at 0 K, so they are approached at 1 K which is certainly not exactly the same as first-principle calculations.

Although the results are not exactly the same, the model is able to predict the SFE value of alloys that are different from the original alloy. Considering that this model was trained with data from FeNiCrAlCu alloy while in this section, the neural network model is used to predict the SFE value of FeNiCrAl alloy. This shows that the machine learning model is capable of predicting alloys other than the alloys in this study.

3.8 FeNiCrAlCu Design Guidance and Suggestions

Designing a high entropy superalloy (HESA) requires consideration of various factors, ranging from elemental determination, atomic percentages, and desired alloy properties. The desired alloy properties in high temperature applications are strength, toughness, oxidation resistance, and good thermal stability at high temperatures. HESA alloys are new alloys developed to provide alternative alloys at high temperatures with properties that are not inferior to super alloys. In a study conducted by Yeh et al [30] the

HESA AlCoCrFeNiTi alloy provides excellent properties such as having a high γ' solvus temperature and having a stable γ-γ' microstructure without any detrimental phase formation. The high temperature strength of HESA is attributed to the high-volume fraction of γ' precipitates, the high degree of solid solution strengthening due to the distortion lattice, and the increase in anti-phase boundary (APB) energy which results in more energy for dislocation pairs to intersect the γ' HESA.

The HESA alloy also has a light density in the range below 8 g/cm3, and raw material costs that are 20% lower than first generation super alloys such as CM247LC. This can be achieved because in HESA, the use of Fe and Ti is increased, while high value elements such as Ni and refractory elements are minimized. The HESA alloy in the study conducted by Yeh [30] showed the prediction of bcc phase formation at low temperatures, but isothermal ageing at 700ºC showed thermal stability, and this is possible due to the nature of the HEA system, namely the phase transformation rate is very sluggish, thus keeping the γ' precipitates stable.

Lattice misfit (δ) is one of the main factors in the process of directional coarsening in γ' precipitates known as "rafting". With a negative value of lattice misfit, it can effectively restrain dislocation climb and produce creep resistance [31]. The role of HESA can be attributed to expanding the lattice misfit in the negative direction, which can be achieved by forming γ and γ' phases not limited to Al, Co, Cr, Fe, Ni, and Ti. In addition, the high activity of Cr and Al in implies continuous Cr_2O_3 and Al_2O_3 that can form rapidly when exposed to oxidative environments at high temperatures.

In HESA FeNiCrAlCu alloy, Ni is the main contributor of the thermal stability of matrix γ and precipitates γ', with the addition of Fe, Cr, and Cu, which can reduce the SFE value, a lower SFE in HESA can be expected. This can be confirmed through the research conducted by Te-Kang Tsao, et al [32] who explained with the optimization parameter of SFE described as $\delta\Gamma_i$, by applying the certain composition [32] to the the model $\Delta_\Gamma^\gamma(x) = \sum_i x_i \delta\Gamma_i$ showed an indication of a decrease in SFE in the fcc matrix due to the addition of elements that decrease SFE into HESA. In addition, elements that contribute to the formation of γ' can significantly increase the APB energy, which can contribute to the strengthening of HESA [33]. The correlation between SFE, creep activation energy, and creep strain rate can be described as the following function [34]:

$$\dot{\epsilon} = A' \left(\frac{\gamma_{sf}}{Gb}\right)^3 (\sigma G)^5 \exp\left(-Q/RT\right)$$

where A' is a constant, γ_{sf} is stacking fault energy, G is shear modulus, b is Burger's vector, Q is activation creep energy and σ is applied stress, so decreasing SFE and increasing Q of HESA can decrease the creep rate [72]. Materials with low SFE, partial dislocations are energetically easier to occur, and the distance between partial dislocations can be increased, resulting in dislocation bowing around the γ' particle will become more difficult, and effectively reduce the creep rate.

Based on the provisions discussed, the optimal composition of the FeNiCrAlCu HESA is sought in order to meet the prerequisites of a HESA, and also to adjust the composition that has a tendency to decrease the SFE value, so as to initiate deformation twinning and reduce the creep rate. The SFE classification used in this study is the result of the classification conducted by Hamada and Vecammen [35], which ranges from low, medium, high as < 25 mJ/m2 ; 25 mJ/m2 < 80 mJ/m2 ; > 80 mJ/m2 respectively. It is important to note that the classification of SFE itself is not absolute, as the specific composition of the alloy, processing methods, can significantly affect the resulting mechanical properties. It is therefore important to evaluate each alloy to determine its mechanical properties and potential applications. However, the method of calculating SFE values has been shown to provide successful results in accounting for alloy and temperature effects [36].

At room temperature, more specifically at 300 K, design guidelines for FeNiCrAlCu HESAs are given. These guidelines are based on the thermodynamic simulation results. Table 2 presents the optimum composition that tends to produce low SFE values, shown in the medium SFE classification.

Table 2 Optimum composition for FeNiCrAlCu

Elemen	Persentase Atom (at %)
Ni	20-25
Cr	15-36
Al	5-20
Cu	9-20
Fe	20-35

Looking at the figure 4-8, Al and Cr significantly affect SFE values, which means it can be considered to be determinant for design guide for FeNiCrAlCu. The same for Fe and Ni, because it's the main component which stabilize the preferred microstructure which is γ and γ' phases.

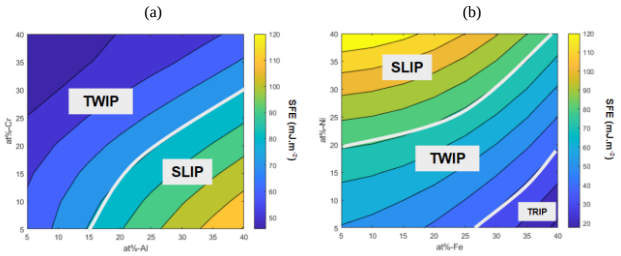

Figure 11 Guide curve for HESA (a) $(FeNiCu)_{100-x-y}Al_xCr_y$ (b) $(AlCrCu)_{100-x-y}Fe_xNi_y$

In order to achieve a low SFE value, and allow for twinning deformation to occur, Figure 11 can be a reference. For example, the alloy with Al-5% and Cr-25% $Fe_{23.3}Ni_{23.3}Cr_{25}Al_5Cu_{23.3}$ composition arrangement will produce an SFE value of 50.25 mJ/m2 and the alloy with Fe-35% and Ni-25% $Fe_{35}Ni_{25}Cr_{13.3}Al_{13.3}Cu_{13.3}$ composition arrangement will produce an SFE value of 60.40 mJ/m2. Both alloys produce relatively low SFE values, and are classified as medium SFE, which is expected to result in deformation twinning. With deformation twinning, the metal alloy will have good toughness, as well as an equilibrium between the ductility and brittleness of the

material, so that it has optimal strength. And the tendency of low SFE can improve creep resistance.

4 Conclusions

1. Temperature and composition affect the SFE value of FeNiCrAlCu alloys. The higher the temperature, the higher the SFE value. The addition of Ni and Al alloys increases the SFE value, while the addition of Fe, Cr, and Cu decreases the SFE. Magnetic influence plays a significant role at low temperatures and decreases with increasing temperature. An increase in mixing entropy can generally decrease the SFE value.
2. Machine learning model built with deeplearning neural network architecture achieved the Root Mean Squared Error of 0.005 for the training and 0.008 for validation
3. The design of FeNiCrAlCu high entropy super alloy aims to obtain SFE value in the range of 25 mJ/m2 < SFE < 80 mJ/m2 to obtain dominant twinning deformation so that cross slip decreases and creep resistance increases. The alloy design must take into account the operating temperature and alloy composition of each element as both factors affect the SFE value. For example, at T = 300 K, the alloy composition can be designed at: Ni 20-25 at%; Cr 15-36 at%; Al 5-20 at%; Cu 9-20 at%; Fe 20-35 at%. In addition, alloys can be designed with the composition configuration $(FeNiCu)_{100-x-y}Al_xCr_y$ and $(AlCrCu)_{100-x-y}Fe_xNi_y$.

References

[1] A. P. Mouritz, "Superalloys for gas turbine engines," *Introduction to Aerospace Materials; Woodhead Publishing: Cambridge, UK*, pp. 251–267, 2012.

[2] C. T. Sims, N. S. Stoloff, and W. C. Hagel, *superalloys II*, vol. 8. Wiley New York, 1987.

[3] P. C. Gasson, "The Superalloys: Fundamentals and Applications RC Reed Cambridge University Press, The Edinburgh Building, Shaftesbury Road, Cambridge, CB2 2RU, UK, 2006. 372pp. Illustrated.£ 80. ISBN 0-521-85904-2.," *The Aeronautical Journal*, vol. 112, no. 1131, p. 291, 2008.

[4] S. Chen, Q. Li, J. Zhong, F. Xing, and L. Zhang, "On diffusion behaviors in face centered cubic phase of Al-Co-Cr-Fe-Ni-Ti high-entropy superalloys," *J Alloys Compd*, vol. 791, pp. 255–264, Jun. 2019, doi: 10.1016/j.jallcom.2019.03.286.

[5] Y.-T. Chen, Y.-J. Chang, H. Murakami, S. Gorsse, and A.-C. Yeh, "Designing high entropy superalloys for elevated temperature application," *Scr Mater*, vol. 187, pp. 177–182, 2020.

[6] E. P. George, D. Raabe, and R. O. Ritchie, "High-entropy alloys," *Nat Rev Mater*, vol. 4, no. 8, pp. 515–534, Jun. 2019, doi: 10.1038/s41578-019-0121-4.

[7] D. Miracle, J. Miller, O. Senkov, C. Woodward, M. Uchic, and J. Tiley, "Exploration and Development of High Entropy Alloys for Structural Applications," *Entropy*, vol. 16, no. 1, pp. 494–525, Jan. 2014, doi: 10.3390/e16010494.

[8] J.-W. Yeh *et al.*, "Nanostructured High-Entropy Alloys with Multiple Principal Elements: Novel Alloy Design Concepts and Outcomes," *Adv Eng Mater*, vol. 6, no. 5, pp. 299–303, May 2004, doi: 10.1002/adem.200300567.

[9] D. B. Miracle and O. N. Senkov, "A critical review of high entropy alloys and related concepts," *Acta Mater*, vol. 122, pp. 448–511, 2017.

[10] Y. Yin *et al.*, "High-temperature age-hardening of a novel cost-effective Fe45Ni25Cr25Mo5 high entropy alloy," *Materials Science and Engineering: A*, vol. 788, p. 139580, 2020.

[11] S. Li *et al.*, "Cost-efficient copper-nickel alloy for active cooling applications," *Int J Heat Mass Transf*, vol. 195, p. 123181, Oct. 2022, doi: 10.1016/j.ijheatmasstransfer.2022.123181.

[12] W. D. Wong-Ángel, L. Téllez-Jurado, J. F. Chávez-Alcalá, E. Chavira-Martínez, and V. F. Verduzco-Cedeño, "Effect of copper on the mechanical properties of alloys formed by powder metallurgy," *Mater Des*, vol. 58, pp. 12–18, Jun. 2014, doi: 10.1016/j.matdes.2014.02.002.

[13] B. Li, E. J. Lavernia, Y. Lin, F. Chen, and L. Zhang, "Spray Forming of MMCs," in *Reference Module in Materials Science and Materials Engineering*, Elsevier, 2016. doi: 10.1016/B978-0-12-803581-8.03884-4.

[14] ASM International, *ASM Handbook Volume 2: Properties and Selection: Nonferrous Alloys and Special-Purpose Materials*, vol. 2. 2002.

[15] P. J. Ferreira and P. Müllner, "A thermodynamic model for the stacking-fault energy," *Acta Mater*, vol. 46, no. 13, pp. 4479–4484, 1998.

[16] T. L. Achmad, W. Fu, H. Chen, C. Zhang, and Z.-G. Yang, "Effects of alloying elements concentrations and temperatures on the stacking fault energies of Co-based alloys by computational thermodynamic approach and first-principles calculations," *J Alloys Compd*, vol. 694, pp. 1265–1279, 2017.

[17] A. Van De Walle and M. Asta, "High-throughput calculations in the context of alloy design," *MRS Bull*, vol. 44, no. 4, pp. 252–256, 2019.

[18] Hojjat Gholizadeh, "The Influence of Alloying and Temperature on the Stacking-fault Energy of Iron-based Alloys," *Montanuniversität Leoben, Chair of Atomistic Modelling and Design of Materials*, May 2013.

[19] Y. H. Zhang, Y. Zhuang, A. Hu, J.-J. Kai, and C. T. Liu, "The origin of negative stacking fault energies and nano-twin formation in face-centered cubic high entropy alloys," *Scr Mater*, vol. 130, pp. 96–99, 2017.

[20] F. Zhang *et al.*, "Polymorphism in a high-entropy alloy," *Nat Commun*, vol. 8, no. 1, p. 15687, 2017.

[21] Z. Y. Wang, D. Han, and X. W. Li, "Competitive effect of stacking fault energy and short-range clustering on the plastic deformation behavior of Cu-Ni alloys," *Materials Science and Engineering: A*, vol. 679, pp. 484–492, Jan. 2017, doi: 10.1016/j.msea.2016.10.064.

[22] J.-Q. Zhao, H. Tian, Z. Wang, X.-J. Wang, and J.-W. Qiao, "FCC-to-HCP Phase Transformation in CoCrNix Medium-Entropy Alloys," *Acta Metallurgica Sinica (English Letters)*, vol. 33, no. 8, pp. 1151–1158, Aug. 2020, doi: 10.1007/s40195-020-01080-6.

[23] A. Dumay, J.-P. Chateau, S. Allain, S. Migot, and O. Bouaziz, "Influence of addition elements on the stacking-fault energy and mechanical properties of an austenitic Fe–Mn–C steel," *Materials Science and Engineering: A*, vol. 483–484, pp. 184–187, Jun. 2008, doi: 10.1016/j.msea.2006.12.170.

[24] J. Yan *et al.*, "Plastic deformation mechanism of CoCrxNi medium entropy alloys," *Materials Science and Engineering: A*, vol. 814, p. 141181, May 2021, doi: 10.1016/j.msea.2021.141181.

[25] K.-T. Park, K. G. Jin, S. H. Han, S. W. Hwang, K. Choi, and C. S. Lee, "Stacking fault energy and plastic deformation of fully austenitic high manganese steels: Effect of Al addition," *Materials Science and Engineering: A*, vol. 527, no. 16–17, pp. 3651–3661, Jun. 2010, doi: 10.1016/j.msea.2010.02.058.

[26] X. Sun, H. Zhang, W. Li, X. Ding, Y. Wang, and L. Vitos, "Generalized Stacking Fault Energy of Al-Doped CrMnFeCoNi High-Entropy Alloy," *Nanomaterials*, vol. 10, no. 1, p. 59, Dec. 2019, doi: 10.3390/nano10010059.

[27] L. Huang, X. Wang, B. Huang, X. Zhao, H. Chen, and C. Wang, "Effect of Cu segregation on the phase transformation and properties of AlCrFeNiTiCux high-entropy alloys," *Intermetallics (Barking)*, vol. 140, p. 107397, 2022.

[28] C. Wang, S. Schönecker, W. Li, Y. Yang, Q.-M. Hu, and L. Vitos, "Twinning pathways in Fe and Fe–Cr alloys from first-principles theory," *Acta Mater*, vol. 215, p. 117094, 2021.

[29] Ammar Zamani, "Pemodelan Stacking Fault Energy Dengan Metode Komputasi Untuk Desain Paduan Entropi Sedang CoCrNiAl dan FeCrNiAl pada Aplikasi Biomedis," 2021.

[30] A. C. Yeh *et al.*, "Developing new type of high temperature alloys–high entropy superalloys," *Int. J. Metall. Mater. Eng*, vol. 1, no. 107, pp. 1–4, 2015.

[31] J. X. Zhang, J. C. Wang, H. Harada, and Y. Koizumi, "The effect of lattice misfit on the dislocation motion in superalloys during high-temperature low-stress creep," *Acta Mater*, vol. 53, no. 17, pp. 4623–4633, Oct. 2005, doi: 10.1016/j.actamat.2005.06.013.

[32] T.-K. Tsao *et al.*, "The high temperature tensile and creep behaviors of high entropy superalloy," *Sci Rep*, vol. 7, no. 1, p. 12658, 2017.

[33] T.-K. Tsao and A.-C. Yeh, "The thermal stability and strength of highly alloyed Ni3Al," *Mater Trans*, vol. 56, no. 11, pp. 1905–1910, 2015.

[34] F. R. N. Nabarro and F. L. de Villiers, "Physics of creep and creep-resistant alloys," *CRC press*, 1995.

[35] N. Chaudhary, A. Abu-Odeh, I. Karaman, and R. Arróyave, "A data-driven machine learning approach to predicting stacking faulting energy in austenitic steels," *J Mater Sci*, vol. 52, pp. 11048–11076, 2017.

[36] Tria Laksana Achmad, "Development of Stacking Fault Energy (SFE) Modelling of Co-based Alloys for Alloy Design," *Tsinghua University*, Apr. 2018.